

Enrichment of lead (Pb) in the Galactic halo*

Wako AOKI,^{1,2} Satoshi HONDA³

¹*National Astronomical Observatory, Mitaka, Tokyo 181-8588*
aoki.wako@nao.ac.jp

²*Department of Astronomical Science, The Graduate University for Advanced Studies,
Mitaka, Tokyo 181-8588*

³*Gunma Astronomical Observatory, Takayama, Agatsuma, Gunma 377-0702*
honda@astron.pref.gunma.jp

(Received 2007 0; accepted 200 0)

Abstract

We have determined lead (Pb) abundances for twelve red giants having $[\text{Fe}/\text{H}]$ between -2.1 and -1.3 , and its upper-limits for two lower metallicity objects, as well as the abundances of lanthanum (La) and europium (Eu). The averages of $[\text{Pb}/\text{Fe}]$ and $[\text{Pb}/\text{Eu}]$ are -0.3 and -0.6 , respectively, and no clear increase of these ratios with increasing metallicity is found. The $[\text{La}/\text{Eu}]$ values are only slightly higher than that of the r-process component in solar-system material. Combining the previous studies for globular clusters, these results suggest little contribution of the s-process to Pb of the field stars studied here, supporting the estimate of Pb production by the r-process from the solar-system abundances.

Key words: Galaxy: halo — nuclear reactions, nucleosynthesis, abundances — stars: abundances — stars: Population II

1. Introduction

Elements heavier than the iron group are mostly synthesized by neutron-capture processes, which are distinguished into the rapid (r-) and slow (s-) processes by the reaction time scale (e.g. Burbidge et al. 1957). The s-process fraction in solar-system material is estimated by the classical or stellar s-process models calibrated for the nuclei that are yielded only by the s-process (e.g. Käppeler et al. 1989, Arlandini et al. 1999). The r-process component is derived by subtracting the s-process one from the solar-system isotopic abundances.

The contributions of the s- and r-processes to Galactic objects are estimated from the abundance ratios of elements that represent the two processes (e.g. Ba/Eu, La/Eu; Truran et al. 1981; McWilliam et al. 1998; Burris et al. 2000). Simmerer et al. (2004) investigated the La/Eu ratio for a large sample of metal-poor stars, and concluded that the contribution of the s-process, with respect to the r-process, increases with increasing metallicity, but large scatter of $[\text{La}/\text{Eu}]$ exists among stars having similar metallicity¹.

Another good probe of the s-process at low metallicity is Pb, one of the heaviest elements including the isotope with magic numbers for proton and neutron (^{208}Pb). The Pb abundances have been measured for many carbon-enhanced objects, which are believed to be affected by mass transfer across binary systems from Asymptotic Giant Branch (AGB) stars, and have been providing a

useful constraint on the s-process in low metallicity AGB stars. In contrast, measurements of Pb abundances for normal (non-carbon-enhanced) stars are quite limited. Travaglio et al. (2001) argued enrichment of Pb in the Galactic halo, thick and thin disks, reporting the Pb abundances for several stars. Their sample, however, includes a star possibly classified as a CH star, and the results for some objects are quite uncertain. Ivans et al. (2006) studied the heavy elements, including Pb, for HD 221170 ($[\text{Fe}/\text{H}] = -2.2$) in detail. Pb abundances of stars in globular clusters were recently determined by Yong et al. (2006) and Yong et al. (2007).

This letter reports our abundance measurements of Pb and other elements for bright metal-poor red giants, which would belong to the Galactic halo. The results are compared with the solar-system s- and r-process abundance ratios as well as that of r-process-enhanced, extremely metal-poor stars.

2. Observation, Analysis and Results

The sample of this study is selected from the list of Burris et al. (2000), who determined abundances of neutron-capture elements like La and Eu, and that of Beers et al. (2000), who studied metallicity and kinematics of metal-poor stars. Bright stars ($V < 10$) were selected for our purpose.

High resolution spectra were obtained for 14 stars given in table 1 with the High Dispersion Spectrograph (HDS; Noguchi et al. 2002) of the Subaru Telescope during several observing runs including a short program in 2007. The resolving power ($R = \lambda/\delta\lambda$) of our observations ranges between 50,000 and 90,000, and the wavelength coverage

* Based on data collected at Subaru Telescope, which is operated by the National Astronomical Observatory of Japan.

¹ $[\text{A}/\text{B}] = \log(N_{\text{A}}/N_{\text{B}}) - \log(N_{\text{A}}/N_{\text{B}})_{\odot}$, and $\log \epsilon_{\text{A}} = \log(N_{\text{A}}/N_{\text{H}}) + 12$ for elements A and B.

Table 1. Object list

Object	$(V - K)_0$	U	V	W
BD+1°2916	3.025	85	-232	14
BD+6°648	2.950	-165	-296	76
BD+30°2611	2.979	-10	-59	-284
HD 3008	3.201	64	-141	54
HD 29574(V* HP Eri)	2.927	-296	-213	-223
HD 74462	2.562	-121	-284	70
HD 141531	2.912	-189	-278	-67
HD 204543	2.716	-11	-130	26
HD 206739	2.495	82	-107	-64
HD 214925	3.269	129	-512	136
HD 216143	2.908	-329	-268	78
HD 220838	2.857	-27	-76	22
HD 221170	2.433	-119	-123	-22
HD 235766	2.396	-305	-260	-4

is 4000–6800 Å, 3700–6400 Å or 3100–4800 Å, depending on observing runs. The data reduction was made with the standard procedure using the IRAF² echelle package (e.g. Aoki et al. 2005). The signal-to-noise ratios of the spectra at the wavelength of the Pb I line used in the analysis (4058 Å) are 85 (per 0.024 Å pixel) or higher.

Chemical abundance analyses were performed using the grid of model atmospheres of Kurucz (1993) with no convective overshooting (Castelli et al. 1997)³. The effective temperatures (T_{eff}) were estimated from photometric colors (SIMBAD and 2MASS; Skrutskie et al. 2006) using the scale of Alonso, Arribas, Martínez-Roger (1999). The reddening was estimated from the dust map of Schlegel, Finkbeiner, Davis (1998) and the interstellar Na D line absorption (Munari & Zwitter 1997) when available. We gave a priority to the $(V - K)_0$ given in table 1 in the effective temperature determination, while other colors were also investigated for comparison purposes. The surface gravity (g), micro-turbulence (v_{turb}), and metallicity ($[\text{Fe}/\text{H}]$) are determined by the LTE analysis for Fe I and Fe II lines, as to obtain no correlation of Fe abundances with line strengths and ionization stages. For the analysis of most objects, we adopted the line list of Ivans et al. (2006). We added Fe I and II lines from O’Brian et al. (1991), Bard, Kock, and Kock (1991), and Fuhr, Martin, Wiese (1988) for relatively metal-rich stars, for which only spectra of the UV–blue range are available. Although a slightly lower $\log g$ value than zero is derived for HD 3008 and HD 214925, we adopted $\log g = 0.0$ for these two stars. This little affects the derived abundance ratios of neutron-capture elements. The stellar parameters adopted for the following analyses are given in table 2. The details of the determinations of stellar parameters will be reported in our future paper (Aoki et al., in preparation). The

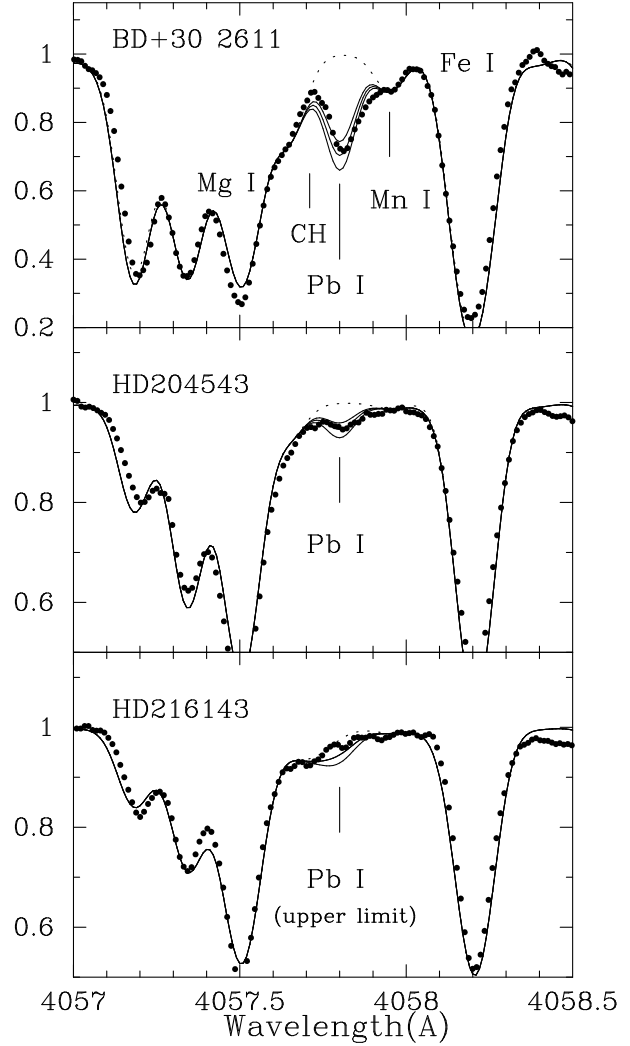


Fig. 1. Comparisons of synthetic spectra for the region including the Pb I 4058 Å line with the observed spectrum. The Pb abundances assumed in the calculations are $\log \epsilon(\text{Pb}) = +0.43 \pm 0.10$ (BD+30°2611), 0.00 ± 0.15 (HD 204543) and $-0.1, -0.3$ (HD 216143) for solid lines, and $-\infty$ for dotted lines. The contamination of the CH line at 4057.7 Å is not severe in the spectra of our non-carbon-enhanced stars.

carbon abundances are estimated from the CH band at 4223 Å. The $[\text{C}/\text{Fe}]$ of our sample ranges between -0.2 and -0.9 , indicating these stars are not carbon-enhanced objects (table 3).

The Pb abundances were determined by fitting synthetic spectra to the observed Pb I 4058 Å line. The line list of Simons et al. (1989) including hyperfine splitting and isotope shifts, which was used by Aoki et al. (2002), was adopted, assuming the solar Pb isotope ratios. We note that the derived abundance is not sensitive to this assumption. Examples of the observed and synthetic spectra are shown in figure 1.

The La and Eu abundances are determined using the line lists of Lawler, Bonvallet, Sneden (2001a) and Lawler et al. (2001b), respectively (see also the appendix of Ivans et al. 2006), including hyperfine splitting. The Eu iso-

² IRAF is distributed by the National Optical Astronomy Observatories, which is operated by the Association of Universities for Research in Astronomy, Inc. under cooperative agreement with the National Science Foundation.

³ <http://wwwuser.oat.ts.astro.it/castelli/grids.html>

tope ratio ($^{151}\text{Eu}/^{153}\text{Eu}$) is assumed to be unity. The La abundance is determined from more than ten lines for all objects, while the Eu lines used are dependent on the targets, because of the differences of the wavelength coverage and the line strengths. The Eu abundances are determined from lines in the red region (6049 Å, 6436 Å, and/or 6645 Å) for most stars. Two lines in the blue region (4129 Å and 4205 Å) are used for objects for which only blue spectra are available. We confirmed that the Eu abundances derived from the blue and red lines agree within 0.13 dex for HD 220838 and HD 221170. The results of the La, Eu and Pb abundances ($\log\epsilon$ values) are given in table 2, and the abundance ratios are given in table 3.

The random errors of the derived abundances are estimated as $\sigma N^{-1/2}$, where σ is the standard deviation of the derived abundances from individual lines and N is the number of lines used. The σ values for Fe and La lines are ~ 0.1 dex or smaller. We adopted σ of Fe I lines as that of Eu, for which five lines or less are available for abundance analyses. The random errors of the Pb abundances are estimated from the fitting of the Pb I line, including the uncertainty of continuum placement. For stars showing a clear Pb I feature (the top panel of figure 1), 0.10 dex is adopted as the fitting error, while 0.15 dex is adopted for stars having weaker features (the middle panel of figure 1). No clear feature is found for HD 216143 (bottom panel of figure 1) and BD+6°648, for which we determined upper limits of Pb abundances.

Errors due to the uncertainty of atmospheric parameters are estimated by calculating abundances changing atmospheric parameters by $\Delta(T_{\text{eff}})=100$ K, $\Delta(\log g)=0.3$ dex, $\Delta([\text{Fe}/\text{H}])=0.2$ dex, and $\Delta(v_{\text{turb}})=0.2$ km s $^{-1}$ for BD+30°2611. These errors are added, in quadrature, to the random errors estimated above, and are given in table 2. The effects of the changes of atmospheric parameters on the abundance ratios of Pb/La, Pb/Eu, and La/Eu are also calculated, and are included in the errors given in table 3. We note that the Pb abundance derived from the neutral species is lower if higher gravity is adopted, while the sign is opposite for La and Eu abundances from ionized species. This results in larger errors in [Pb/La] and [Pb/Eu] than those in [La/Eu].

A comparison of our abundance results for HD 221170 with those of Ivans et al. (2006) shows 0.1-0.2 dex differences in the abundances of Fe, La, Eu and Pb, which are, at least qualitatively, explained by the differences of adopted atmospheric parameters ($\Delta T_{\text{eff}}=90$ K and $\Delta \log g=0.5$ dex). The abundances of HD 141531 are determined by the present work for the same spectrum as used by Yong et al. (2006). The results agree within 0.05 dex between the two measurements, adopting almost the same stellar parameters.

3. Discussion and concluding remarks

The top panel of figure 2 shows [Pb/Fe] as a function of [Fe/H] for the field stars of our sample and for globular cluster stars. The Pb of our sample is underabun-

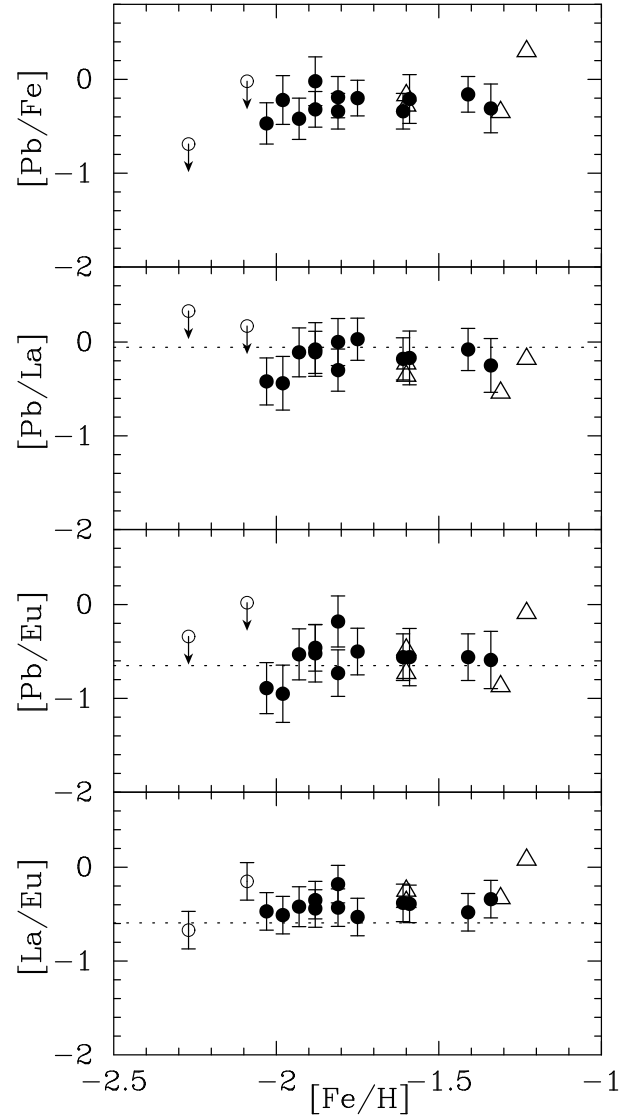


Fig. 2. Abundance ratios of the neutron capture elements La, Eu, and Pb as functions of [Fe/H]. Circles indicate our results. Open circles mean the result for the two objects for which only an upper limit of the Pb abundance is determined. Open triangles are the results for the globular clusters M4, M5, M13, and NGC 6752 by Yong et al. (2006) and Yong et al. (2007). The dotted lines in the lower three panels show the abundance ratios of the solar-system r-process components (Simmerer et al. 2004).

dant, and the abundance scatter is small: the average of [Pb/Fe] is -0.27 and the standard deviation is 0.12 dex (table 4). This result indicates no rapid increase of Pb in this metallicity range in our sample. The open triangles in this panel present the averages of Pb abundance ratios of stars in the globular clusters M 4, M 5, M 13 and NGC 6752 (Yong et al. 2006; Yong et al. 2007). While the [Pb/Fe] of three clusters agrees with that found for our field stars, the value of M 4 ($[\text{Fe}/\text{H}]=-1.23$) is higher by 0.5 dex. The high Pb abundance ratio should be the result of the large s-process contribution to this cluster (Ivans et al. 1999).

In order to investigate the origins of Pb in the field stars, we depict the abundance ratios of Pb/La, Pb/Eu and La/Eu in the lower three panels of figure 2. The dotted lines in these panels mean the abundance ratios of the r-process component in solar-system material (table 4) determined by Simmerer et al. (2004). The Pb/Eu and La/Eu of the s-process component are much higher than those of the r-process component. Hence, the agreement of [Pb/Eu] of the field stars with that of the solar-system r-process component implies that the r-process is the dominant source of Pb in our sample, and the contribution of the s-process is small if any.

The little contribution of the s-process to our sample is also suggested by the La/Eu ratios. The La and Eu abundances of a large sample of metal-poor stars were investigated by Simmerer et al. (2004). Seven stars among our objects are included in their sample, and the [La/Eu] values measured by the two studies agree well. However, their sample also includes stars having relatively high La/Eu ratios ([La/Fe] ~ -0.2) in this metallicity range, and they concluded the existence of a spread in the level of s-process enrichment. Measurements of Pb for the stars having higher La/Eu ratios are desirable. It should be noted, however, that most of such stars in their sample have relatively high temperature, and measurements of Pb abundances are relatively difficult.

Simmerer et al. (2004) argued a correlation between the La/Eu ratio and the kinematic properties of the objects, suggesting that “high velocity stars” having high U and W , or low V , show low La/Eu ratios. The kinematics data of our objects taken from Beers et al. (2000) are given in table 1. They show the characteristics of “high velocity stars”, with a possible exception of HD 220838, supporting the arguments of Simmerer et al. (2004).

The above discussion is based on the r-process component in solar-system material estimated by Simmerer et al. (2004). However, the Pb productions by the s- and r-processes are still very uncertain. Indeed, the detailed abundance studies for r-process-enhanced, extremely metal-poor stars reported significantly lower Pb abundance ratios (Plez et al. 2004; Frebel et al. 2007). For instance, CS 31082-001 has [Pb/Eu] of -1.28 (Plez et al. 2004; Hill et al. 2002), 0.63 dex lower than that of the solar-system r-process component (table 4). If we adopt this as the abundance ratio of the r-process contribution (assuming Eu is entirely the r-process origin), only 20% of Pb of our sample ($\langle [\text{Pb}/\text{Eu}] \rangle = -0.59$) is from the r-process and the remaining 80% is the s-process origin. In contrast, the average of [La/Eu] of our sample ($\langle [\text{La}/\text{Eu}] \rangle = -0.41$) is only slightly higher than that of CS 31082-001 ([La/Eu] = -0.52). If similar estimate to Pb is applied, 22% of La originates from the s-process. These estimates results in the Pb/La ratios of the “s-process component” of the field stars to be $[\text{Pb}/\text{La}]_s = \langle [\text{Pb}/\text{La}] \rangle + \log(0.80/0.22) = 0.38$.

Thus, an alternative interpretation for our result is that the r-process yield of Pb is as low as that found in the r-process-enhanced extremely metal-poor stars, while the Pb production with respect to La by the s-process at low

metallicity is quite efficient. An efficient synthesis of ^{208}Pb at low metallicity is predicted by the s-process calculations for AGB models with ^{13}C pocket (e.g. Busso et al. 1999). However, the decrease of Pb/La ratios (possibly by one dex) with increasing metallicity, which is expected from such models, is not found in our sample. Another difficulty of this interpretation is the abundance ratios of M 4 stars. While the high La and Pb abundances of this cluster indicate large contributions of the s-process, the $\langle [\text{Pb}/\text{La}] \rangle$ of this cluster (table 4) is significantly lower than the $[\text{Pb}/\text{La}]_s$ estimated above. That is, assuming large contributions of the s-process to our field stars requests an unnatural assumption that the s-process yields are significantly different between field stars and globular cluster objects.

Our conclusion here is that Pb, as well as other neutron-capture elements, in a majority of halo stars in the metallicity range of $[\text{Fe}/\text{H}] < -1.3$ primarily originated from the r-process. This supports the Pb production by the r-process estimated from solar-system abundances (e.g. Burris et al. 2000; Simmerer 2004), and suggests that the Pb abundance of r-process-enhanced, extremely metal-poor stars (e.g. CS 31082-001) is anomalously low. Such diversity of Pb production by the r-process is recently argued by Wanaajo (2007). However, given the fact that some stars having high La/Eu ratios are known in this metallicity range, further measurements of Pb abundances for a larger sample are strongly desired.

References

- Alonso, A., Arribas, S., & Martínez-Roger, C. 1999, *A&AS*, 140, 261
- Aoki, W., Ryan, S. G., Norris, J. E., Beers, T. C., Ando, H., & Tsangarides, S. 2002, *ApJ*, 580, 1149
- Aoki, W., et al. 2005, *ApJ*, 632, 611
- Arlandini, C., Käppeler, F., Wisshak, K., Gallino, R., Lugaro, M., Busso, M., & Straniero, O. 1999, *ApJ*, 525, 886
- Bard, A., Kock, A., & Kock, M. 1991, *A&A*, 248, 315
- Beers, T. C., Chiba, M., Yoshii, Y., Platais, I., Hanson, R. B., Fuchs, B., & Rossi, S. 2000, *AJ*, 119, 2866
- Burbidge, E. M., Burbidge, G. R., Fowler, W. A., & Hoyle, F. 1957, *Reviews of Modern Physics*, 29, 547
- Burris, D. L., Pilachowski, C. A., Armandroff, T. E., Sneden, C., Cowan, J. J., & Roe, H. 2000, *ApJ*, 544, 302
- Busso, M., Gallino, R., & Wasserburg, G. J. 1999, *ARA&A*, 37, 239
- Castelli, F., Gratton, R. G., & Kurucz, R. L. 1997, *A&A*, 318, 841
- Frebel, A., Christlieb, N., Norris, J. E., Thom, C., Beers, T. C., & Rhee, J. 2007, *ApJL*, 660, L117
- Fuhr, J.R., Martin, G.A., & Wiese, W.L. 1988, *J. Phys. Chem. Ref. Data*, 17, suppl. 4
- Hill, V., et al. 2002, *A&A*, 387, 560
- Ivans, I. I., Simmerer, J., Sneden, C., Lawler, J. E., Cowan, J. J., Gallino, R., & Bisterzo, S. 2006, *ApJ*, 645, 613
- Ivans, I. I., Sneden, C., Kraft, R. P., Suntzeff, N. B., Smith, V. V., Langer, G. E., & Fulbright, J. P. 1999, *AJ*, 118, 1273
- Käppeler, F., Beer, H., & Wisshak, K. 1989, *Reports of Progress in Physics*, 52, 945
- Kurucz, R. 1993, *ATLAS9 Stellar Atmosphere Programs and*

Table 2. Elemental Abundances Results

Object	model parameters				abundances results							
	T_{eff}	$\log g$	v_{turb}	[Fe/H]	$\log \epsilon(\text{Fe})$	error	$\log \epsilon(\text{La})$	error	$\log \epsilon(\text{Eu})$	error	$\log \epsilon(\text{Pb})$	error
BD+1°2916	4200	0.4	1.8	-1.9	5.57	0.18	-0.87	0.12	-1.22	0.14	-0.20	0.19
BD+6°648	4400	0.9	2.2	-2.1	5.36	0.19	-0.95	0.12	-1.50	0.16	<0.0	...
BD+30°2611	4250	0.5	1.9	-1.5	6.04	0.18	-0.27	0.12	-0.49	0.14	0.43	0.19
HD 3008	4150	0.0	2.4	-1.8	5.52	0.19	-1.02	0.14	-1.30	0.16	-0.35	0.22
HD 29574	4250	0.3	1.9	-1.8	5.64	0.18	-0.63	0.12	-0.90	0.14	-0.15	0.19
HD 74462	4600	1.5	1.3	-1.4	6.11	0.18	-0.18	0.12	-0.54	0.14	0.35	0.26
HD 141531	4300	0.7	1.6	-1.7	5.84	0.18	-0.55	0.12	-0.87	0.14	0.05	0.19
HD 204543	4600	1.0	2.2	-1.9	5.64	0.19	-0.78	0.12	-1.30	0.16	0.00	0.22
HD 206739	4600	1.5	1.6	-1.6	5.86	0.18	-0.41	0.12	-0.72	0.18	0.20	0.26
HD 214925	4050	0.0	2.1	-2.0	5.42	0.18	-0.86	0.12	-1.09	0.20	-0.50	0.22
HD 216143	4450	0.8	2.3	-2.3	5.18	0.19	-1.21	0.12	-1.24	0.15	<-0.10	...
HD 220838	4300	0.6	1.8	-1.8	5.70	0.18	-0.76	0.12	-0.93	0.16	0.05	0.19
HD 221170	4600	1.5	1.9	-2.1	5.47	0.18	-0.54	0.12	-0.73	0.14	-0.20	0.26
HD 235766	4650	1.2	1.9	-1.8	5.57	0.18	-0.60	0.12	-0.86	0.14	0.10	0.26

- 2 km/s grid. Kurucz CD-ROM No. 13. Cambridge, Mass.:
 Smithsonian Astrophysical Observatory, 1993., 13,
 Lawler, J. E., Bonvallet, G., & Sneden, C. 2001a, ApJ, 556,
 452
 Lawler, J. E., Wickliffe, M. E., den Hartog, E. A., & Sneden,
 C. 2001b, ApJ, 563, 1075
 McWilliam, A. 1998, AJ, 115, 1640
 Munari, U., & Zwitter, T. 1997, A&A, 318, 269
 Noguchi, K., et al. 2002, PASJ, 54, 855
 O'Brian, T. R., Wickliffe, M. E., Lawler, J. E., Whaling,
 J. W., & Brault, W. 1991, Journal of the Optical Society
 of America B Optical Physics, 8, 1185
 Plez, B., et al. 2004, A&A, 428, L9
 Simons, J.W., Palmer, B.A., Hof, D.E., & Oldenborg, R.C.
 1989, J. Opt. Soc. Am. B., 6, 1097
 Schlegel, D.J., Finkbeiner, D.P., & Davis, M. 1998, ApJ, 500,
 525
 Simmerer, J., Sneden, C., Cowan, J. J., Collier, J., Woolf,
 V. M., & Lawler, J. E. 2004, ApJ, 617, 1091
 Skrutskie, M. F., et al. 2006, AJ, 131, 1163
 Travaglio, C., Gallino, R., Busso, M., & Gratton, R. 2001,
 ApJ, 549, 346
 Truran, J. W. 1981, A&A, 97, 391
 Wanajo, S. 2007, ApJL, 666, L77
 Yong, D., Aoki, W., Lambert, D. L., & Paulson, D. B. 2006,
 ApJ, 639, 918
 Yong, D., Lambert, D. L., Paulson, D. B., & Carney, B. W.
 2007, ApJ, in press, arXiv:0710.2367

Table 3. Elemental Abundances Ratios

Object	[Fe/H]	[C/Fe]	[Pb/Fe]	error	[Pb/La]	error	[Pb/Eu]	error	[La/Eu]	error
BD+1°2916	-1.88	-0.66	-0.32	0.19	-0.11	0.22	-0.46	0.25	-0.35	0.20
BD+6°648	-2.09	-0.15	< -0.02	< 0.17	< 0.02	-0.15	0.20
BD+30°2611	-1.41	-0.78	-0.16	0.19	-0.08	0.22	-0.56	0.25	-0.48	0.20
HD 3008	-1.93	-0.51	-0.42	0.22	-0.11	0.26	-0.53	0.27	-0.42	0.21
HD 29574	-1.81	-0.83	-0.34	0.19	-0.30	0.22	-0.73	0.25	-0.43	0.20
HD 74462	-1.34	-0.40	-0.31	0.26	-0.25	0.29	-0.59	0.31	-0.34	0.20
HD 141531	-1.61	-0.58	-0.34	0.19	-0.18	0.22	-0.56	0.25	-0.38	0.20
HD 204543	-1.81	-0.63	-0.19	0.22	0.00	0.25	-0.18	0.27	-0.18	0.20
HD 206739	-1.59	-0.25	-0.21	0.26	-0.17	0.29	-0.56	0.31	-0.39	0.20
HD 214925	-2.03	-0.81	-0.47	0.22	-0.42	0.25	-0.89	0.27	-0.47	0.20
HD 216143	-2.27	-0.37	< -0.69	< 0.33	< -0.34	-0.67	0.20
HD 220838	-1.75	-0.49	-0.20	0.19	0.03	0.22	-0.50	0.25	-0.53	0.20
HD 221170	-1.98	-0.61	-0.22	0.26	-0.44	0.29	-0.95	0.31	-0.51	0.20
HD 235766	-1.88	-0.66	-0.02	0.26	-0.08	0.29	-0.52	0.31	-0.44	0.20

Table 4. Abundance ratios of neutron-capture elements

Object	Ref.*	[Pb/Fe]	[Pb/La]	[Pb/Eu]	[La/Eu]
field stars (12 objects) [†]	1	-0.27 (0.12)	-0.18 (0.15)	-0.59 (0.20)	-0.41 (0.09)
M 4 stars (12 objects) [†]	2	0.30 (0.07)	-0.18 (0.06)	-0.09 (0.09)	0.08 (0.06)
s-process (solar-system)	3		0.022	1.471	1.449
r-process (solar-system)	3		-0.057	-0.650	-0.593
CS 31082-001	4	0.35	-0.76	-1.28	-0.52

* References: (1)This work; (2)Yong et al. (2007); (3)Simmerer et al. (2004); (4)Hill et al. (2002) and (Plez et al. 2004).

[†] Averages and standard deviations of abundance ratios.